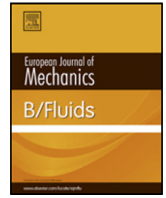




Contents lists available at ScienceDirect

European Journal of Mechanics B/Fluids

journal homepage: www.elsevier.com/locate/ejmflu

Computational fluid dynamics analysis of wall shear stresses between human and rat nasal cavities

Y. Shang, J.L. Dong, K. Inthavong*, J.Y. Tu

School of Engineering - Mechanical & Automotive, RMIT University, PO Box 71, Bundoora, VIC 3083, Australia

ARTICLE INFO

Article history:
Available online xxxx

Keywords:
Wall shear stress
CFD
Nasal cavity
Surface unwrapping

ABSTRACT

Toxicology studies often use laboratory animals as surrogates for human subjects because of the relatively similar nasal anatomy that allows data extrapolation between species. An understanding of nasal airflow patterns, particularly wall shear stress can help better understand the causes of toxicant distribution and local dosimetry. A laminar, steady state flow was used to simulate light inhaled air. The WSS produced inside a human nasal cavity was compared with a rat nasal cavity. The results showed that averaged WSS was highest in the anterior nasal region, i.e. vestibule (rat - 755 mPa and human - 153 mPa). In the human model, the lower septal wall, and nasopharynx region also exhibited high WSS regions. Local high WSS regions on the nasal cavity wall were identified by plotting the WSS distribution as 3D contour maps on a normalised 2D domain. This visualisation technique displays peaks for locally high WSS values which were primarily caused by the airway geometry intruding into the airflow paths and causing high shear. Velocity vectors on the 2D domain also correlated high WSS with flow acceleration that was caused by a reduction in the cross-sectional area of a local region in the nasal passage.

Crown Copyright © 2016 Published by Elsevier Masson SAS. All rights reserved.

1. Introduction

The nasal cavity serves as a front line defence for the lungs by filtering foreign airborne contaminants, and conditioning the inhaled air. The delicate lungs and olfactory regions are vulnerable to airborne contaminants caused by exposure to the inhaled air. Furthermore, the nasal epithelium is continuously subjected to shearing forces from the moving air passing over the nasal walls, which is the wall shear stress (WSS). Excessive WSS can lead to mechano-receptors in the epithelial lining of the nasal cavity triggering mucus secretion from the goblet cells [1]. This was also confirmed by Even-Tzur et al. [2] and Davidovich et al. [3] whom showed the occurrence of significant mucus secretion increase in response to WSS stimuli compared with unstressed conditions.

The compact size and complex nasal cavity geometry makes in-vivo nasal airflow studies challenging leading preference for in-vitro experiments in nasal airway cast models. Hahn et al. [4] provided detailed velocity measurements in a 20 enlarged right-nasal cavity. Both inhalation and exhalation breathing at five cross-sectional planes were measured using a hot-film anemometer. It was found that 50% of inhaled air flowed through the combined

middle and inferior passage and 14% through the olfactory region for all studied flow rates. Schreck et al. [5] performed pressure measurements, flow visualisation and hot-wire anemometry studies using a 3 enlarged model. Significant pressure drop was observed at the anterior nasal cavity during inhalation, and a number of vortices were formed posterior to the nasal valve. Kelly et al. [6] conducted detailed particle image velocimetry (PIV) measurements over 2D lateral fields and sampled parallel planes through the right chamber of a nasal cavity. The resulting vector plots demonstrated airflow was laminar at 125 ml/sec and peak velocities occurred at the nasal valve and the inferior airway.

To obtain very detailed data, computational fluid dynamics (CFD) methods are widely applied [7–12]. Keyhani et al. [13] simulated airflow in the right chamber of a healthy adult nose under quiet breathing conditions, and showed that nearly 30% of the inhaled air flowed through the inferior turbinate region, and 10% through the olfactory region. Wen et al. [14] detailed the airflow features through CFD simulations adopting laminar steady flow conditions, and demonstrated the differences between the left and right chambers. Other CFD studies found general agreement of the persistent gross flow features, including high velocities in the constrictive nasal valve region and close to the septum walls, and vortex formations posterior to the nasal valve and olfactory regions Ishikawa et al. [15]; Garcia et al. [16]; Horschler et al. [17], Xi et al. [18]. Elad et al. [1] presented WSS distributions based on a simplified human nose-like model, which showed

* Corresponding author.

E-mail address: kiao.inthavong@rmit.edu.au (K. Inthavong).

Table 1
General information of rat and human geometries.

	Nasal volume (mm ³)			Hydraulic diameter (mm)		
	Left chamber	Right chamber	Total	Nostril	Choanae	Nasopharynx
Rat RNC01						
– Without sinus	210	230	440	–	–	–
– With sinus	226	247	473	0.784	2.76	2.56
Human NC04						
– Without sinus	14 109	11 201	25 310	–	–	–
– With sinus	14 689	16 108	30 797	11.3	16.1	9.0

Table 2
Comparisons of areas of nine major anatomical regions for rat and human.

Region	% of total surface area			% of total surface area		
	Surface area of rat RNC01 (mm ²)	Current study	Literature	Surface area of human NC04 (mm ²)	Current study	Literature
Vestibule	133	5.4%	3.5 ^b , 4.4 ^b , 4.0 ^d	1 640	7.3	8.2 ^b , 6.2 ^d
Upper passage	119	4.8%		664	2.9	
Middle passage	242	9.8%		5 252	23.3	
Lower passage	137	5.6%		5 077	22.6	
Olfactory	1288	52.4%	42 ^b , 41 ^c , 51 ^a	1 887	8.4	9.5 ^b
Upper septum	151	6.1%		2 053	9.1	
Lower septum	157	6.4%		2 056	9.1	
Pharynx	88	3.6%		1 216	5.4	
Maxillary sinus	143	5.8%		2 675	11.9	
Total (mm ²)	2458	100%		25 518	100	

^a Gross et al. [29].^b Schroeter et al. (2008).^c Garcia and Kimbell [21].^d Schroeter et al. [26].

high WSS regions at the narrowest passages such as the nasal valve region, and the anterior middle turbinate. Doorly et al. [19] approximated WSS distributions on the nasal septum and observed a flow stagnation point below the leading edge of the turbinate together with high WSS regions. More recently studies have begun looking at exploiting the olfactory region for nanoparticle intrusion into the blood stream to bypass the tightly bounded blood–brain-barrier [20–22].

In toxicology studies, laboratory animals (mostly rat or mice) are widely used as surrogates for human subjects due to the relatively similar nasal anatomy to allow data extrapolation between species. Morgan et al. [23] studied inspiratory nasal airflow in transparent acrylic replicas of rat and monkey nasal passages using a water-dye siphon system. Based on dye streamlines, the anterior rat nasal airway model was considered to play an important role in local mixing of inhaled air. Garcia et al. [21] numerically modelled nanoparticle deposition in the olfactory region of a rat, which was largely dependent on the flow patterns. Their results indicated that only 20% of inhaled air was diverted to the olfactory region, while most the flow exited the nasopharynx. Meanwhile, site-specific nasal lesions have been recognised in rats after inhalation exposure to chemical toxicants such as formaldehyde [24–26].

Toxicant distribution and dosage within nasal cavities is highly dependent on the combined effects of anatomical structure and airflow patterns, especially at the air–wall interface. Therefore, an understanding of nasal airflow patterns, particularly wall shear stress, for both laboratory animals and human can help to reduce uncertainties during in-vivo exposure studies and advance the data extrapolation from rat to human. In particular is the predictions of particle deposition in the olfactory region. Despite extensive experimental and numerical investigations of nasal cavity airflows in the literature, no WSS distribution analysis has been conducted for the rat nasal model, and therefore there is no WSS comparison between human and rat models. Furthermore, visualisation of WSS distributions on the entire nasal cavity surface remains challenging due to the highly overlapping 3D nasal structure, and possible information of local concentrated stresses can be hidden

behind these structures (e.g. the shell-like turbinates). To fulfil the knowledge gap on the WSS distribution comparison between human and rat nasal cavities, realistic computational models of the nose were reconstructed from CT images, and numerical comparison of the airflow patterns and WSS distributions were performed under a steady state laminar flow. A technique to visualise the 3D domain onto a 2D space was presented to visualise the WSS distribution over the entire nasal cavity surface.

2. Methods

2.1. Nasal cavity models

The remarkable nasal functions are accomplished by a delicate geometrical structure which balances the convection of airflow with heat and mass transfer by diffusion, while distributing mucus secretion within the nasal cavity. Thus, the reconstruction of rat and human nasal cavity geometries need to be well addressed. In this study, the rat nasal model was reconstructed from CT images (resolution 768 px × 768 px) of a 400 g Sprague-Dawley rat with resolution of 0.05 mm. Similarly, the human nasal model was reconstructed from CT images (resolution 512 px × 512 px) of a 48-year-old Asian male, with resolution 0.5 mm. The human model has exhibited a slightly deviated septum and has been used in previous studies Shang et al. [27]; Dong et al. [28]. The external facial features were included to ensure realistic inhalation at the nostrils which have shown to affect the downstream flow inside the nasal cavity Xi et al. [11]; Shang et al. [27]; Doorly et al. [19].

Fig. 1 presents the reconstructed nasal cavity models for rat (labelled RNC01) and human (labelled NC04), inclusive of the paranasal sinus, pharynx and larynx anatomy. Cross-sectional slices with nasal cavity dimensions are given in Fig. 1(b) to highlight the size and shape difference between the two species. The main differences include: the length of the main nasal chamber, rat model was 3.6 cm long while the human model was 9.8 cm; there were many turbinate structures producing highly curved cross-section slices in the rat model (slice b-b) while in

Download English Version:

<https://daneshyari.com/en/article/4992373>

Download Persian Version:

<https://daneshyari.com/article/4992373>

[Daneshyari.com](https://daneshyari.com)